A Multiplexing Off-Line LED Driver Achieves High Power Factor and Flicker-Free Operation

Peng Fang
Dept. of Electrical Engineering
University of Minnesota Duluth
Duluth, U.S.A
fangp@d.umn.edu

Yan-Fei, Liu, Paresh C. Sen
Dept. of Electrical and Computer Engineering
Queen's University
Kingston, Canada
yanfei.liu@queensu.ca, senp@queensu.ca

***Abstract*—Although a single-stage off-line LED driver can achieve low cost and high efficiency, the notorious double-line-frequency flicker issue with a single-stage LED driver limits its usage in high-quality lighting applications. To solve lighting flicker, multiplexing operation is proposed in this paper. One switching cycle is further divided into two portions, namely phase one and phase two, which produces a main output voltage and an opposite ripple voltage. The main and the opposite ripple voltage are connected in series to form the LED voltage, which is a DC because of ripple cancellation. Therefore, a DC LED current can be produced and achieves flicker-free LED driving performance. A 7.5W experimental prototype had been built and tested to verify the design concept.**

I. Introduction

Light Emitting Diode (LED) lighting has gained significant popularity in residential, commercial, automotive and many other general lighting applications. Compared to traditional lighting technologies, such as incandescent and fluorescent lighting, LED lighting is more energy saving, reliable and environmentally friendly. The global LED lighting market is expected to reach \$58 billion US dollars in 2022 with a growth rate of around 13% between 2017 and 2022 [1]. Undoubtedly, LED lighting will become a dominant lighting choice in the near future.

Although LED lighting technology is promising, some challenges need to be overcome to maximize the benefit of using it. A specially designed power supply, LED driver, is required to power the LED load and regulate the current. The intrinsic low internal resistance of an LED load makes it prone to light flickering, especially when an LED load is driven by an off-line LED driver that needs to meet power factor requirements from EnergyStar [2]. This requires power factor correction (PFC) for any off-line LED drivers have higher than 5W rated power, 0.7 PF for residential and 0.9 PF for commercial usage.

Fig. 1 shows the critical line cycle waveforms when a unity power factor is implemented. The input current follows the input voltage and the AC input power waveform is sinusoidal with a DC bias at half of the peak value. To achieve flicker-free LED driving, the expected output power is equal to the average AC input power. Therefore, there is imbalanced energy between the AC input and the LED load output at double-line-frequency. The imbalanced energy further generates a ripple voltage on the output of the PFC stage at the same frequency. In a single-stage off-line LED driver, the ripple voltage is directly applied to its LED load. Because of very low internal resistance of an LED load, the ripple voltage causes an exaggerated ripple LED current, also at double-line-frequency. The ripple LED current is almost proportionally presented as lighting fluctuation - flicker. Although flicker at higher than 70Hz frequency is usually invisible, it is proven to be harmful and can lead to many uncomfortable symptoms such as: headaches, vision impairments, and even seizures [3]. A two-stage LED driver can naturally achieve flicker-free LED driving performance. The ripple voltage generated by the PFC stage is filtered by a second stage DC-DC converter. Therefore, a DC LED voltage can be generated and used to drive a LED load to achieve flicker-free performance. Because of the additional power stage, two-stage LED drivers are usually lower in efficiency and higher on component costs. Especially in low power applications (below 10W), it is undesirable to add further cost.

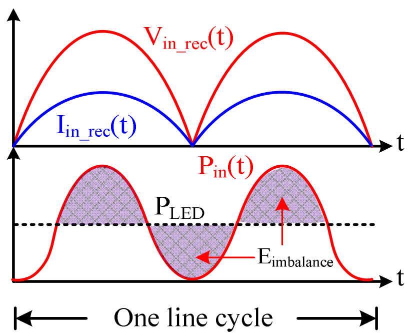

Fig. 1 Typical line cycle waveforms of a single-stage LED driver

A variety of LED driving methods have been presented attempts to improve efficiency, reduce component cost and achieve flicker-free LED driving performance. Some methods improve the control strategy of LED drivers. For example, the harmonic input currents injection method [4]-[6] had been proposed to reduce double-line-frequency imbalanced energy existing in a single-stage LED driver. Therefore, the ripple LED current is reduced to alleviate lighting flicker. Also, the primary side current estimation methods [7]-[10] had been proposed to achieve primary side control, which reduces component costs and improves reliability. Other methods focus on improving the power stage structure of LED drivers. An example of this is the energy buffering technologies [11]-[14] which had been proposed to balance energy difference between AC input and

978-1-7281-0395-2/19/\$31.00 ©2019 IEEE

LED output with a bi-directional DC-DC converter. Further, the two-stage integrated methods [15]-[19] had been proposed to share components between the first PFC stage and the second DC-DC stage, which can reduce component cost.

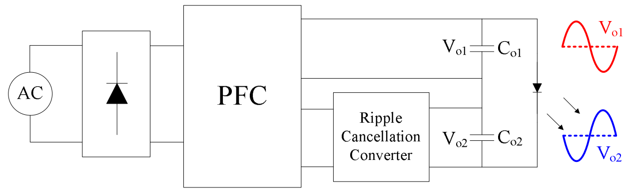

Fig. 2 Generic structure of ripple cancellation LED driver [20] – [25]

The concept of ripple cancellation LED drivers [20]-[25] is shown in Fig. 2. A main PFC is used to transfer energy from AC input to LED output and achieve power factor correction. A separate ripple cancellation converter is used to produce an opposite double-line-frequency ripple voltage. By connecting these two voltages in series, the main ripple voltage is canceled by the opposite ripple voltage and a DC LED voltage is produced to achieve flicker-free LED driving performance. An energy channeling LED driver, which is also based on the concept of ripple cancellation, was proposed in [25]. It can achieve flicker-free operation while maintaining a low component cost. The drawbacks of this design include undesired AC input current zero-crossing distortion as well as limited input voltage range. It is difficult to optimize operation under both the high and the low line inputs with one set of design parameters. A multiplexing energy channeling (MEC) LED driver is a new method proposed in this paper. Under this operation, the AC input current zero-crossing distortion is eliminated, and the design can work under an extensive input voltage range.

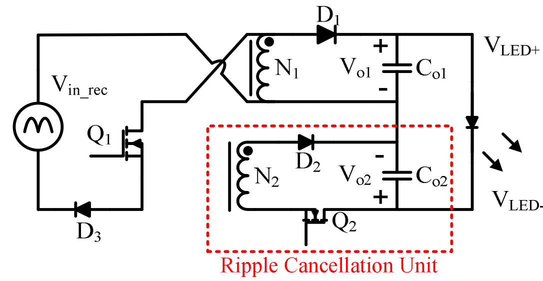

Fig. 3 Circuit implementation of the proposed multiplexing energy channeling LED driver based on Buck-Boost topology.

The remaining of this paper is organized as follows. Section II discusses the concept and operating principle of the MEC LED driver; Section III discusses the control strategy of the LED driver; The experimental result of the designed prototype is presented in section IV followed by the conclusion in section V.

II. Operating Principles

Fig. 3 shows a Buck-Boost topology-based implementation of the proposed MEC LED driver. The same concept can be implemented with other current-fed topologies, such as Flyback, and Boost. Compared to a conventional Buck-Boost LED driver, the proposed MEC LED driver contains an additional ripple cancellation unit (RCU), which is highlighted in red dash box. The RCU is active during the phase two operation, through which an opposite ripple voltage is produced. There is an additional diode, D_3, to ensure unidirectional current flow which

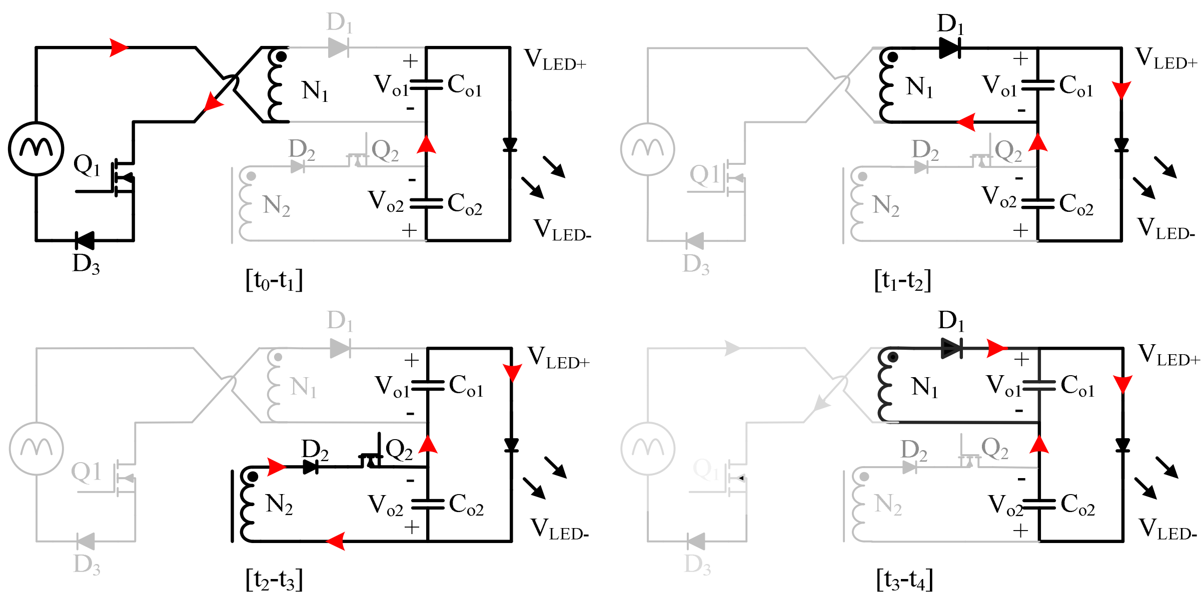

Fig. 4. One switching cycle operation of the proposed multiplexing energy channeling LED driver

will be explained in the later part of this section. It will also be explained that the D_2, Q_2 and D_3 have very low voltage stresses (around 20V) and can be implemented with low voltage rating devices to maintain an overall low cost. It should be noted in Fig. 2. that the output V_{o2} is negative, which is indicated with the top plate of C_{o2} being negative and the bottom plate of C_{o2} being positive. The switching operation of the proposed LED driver is shown in Fig. 4. and the key switching waveforms are shown in Fig. 5. The detailed switching operation in each time interval will be discussed as follows.

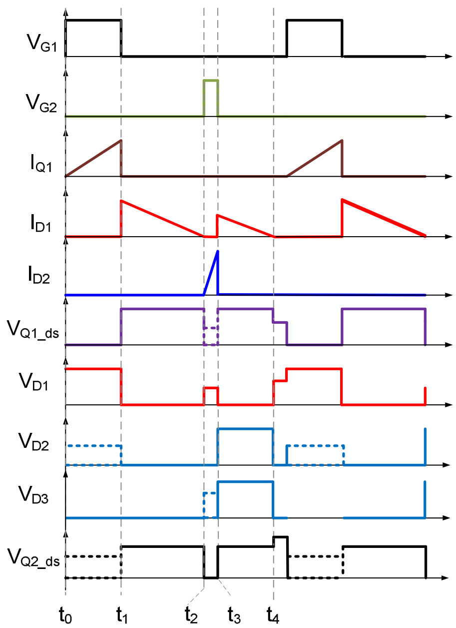

Fig. 5. Key switching waveforms of the proposed multiplexing energy channelling LED driver.

A. Time Interval [t_0-t_1]

A switching cycle starts at time t_0 when the MOSFET Q_1 is turned on. The inductor is charged by the rectified AC input. The switching current in winding N_1 starts rising from zero and increases linearly with the turn on time. It peaks at time t1 right before Q_1 is turned off. The switching current in MOSFET Q_1 at time t_1, I_{Q1_t1}, can be expressed as:

$$I_{Q_1\_t_1} = \frac{V_{in\_rec} \times (t_1 - t_0)}{L_{N1}} \tag{1}$$

In (1), L_{N1} represents the inductance of the winding N_1. The averaged current drawn from AC input during phase one operation, I_{in_avg}, can be expressed as:

$$I_{in\_avg} = \frac{I_{Q1\_t_1} \times (t_1 - t_0)}{2T_s} \tag{2}$$

Further combining (1) and (2) yields:

$$I_{in\_avg} = \frac{V_{in} \times (t_1 - t_0)^2}{2 \times T_s \times L_{N1}} \tag{3}$$

As both the terms (t_1-t_0) and T_s are constant in a half line cycle, I_{in_avg} is therefore proportional to the input voltage and power factor correction is performed.

The diode D_1 is reverse biased and the voltage stress on D_1 during this time interval can be expressed as:

$$V_{D_1[t_0-t_1]} = V_{o1} + V_{in\_rec} \tag{4}$$

The voltage across the winding N_2 can be expressed as:

$$V_{N_2[t_0-t_1]} = V_{in\_rec} \times \frac{N_2}{N_1} \tag{5}$$

If the voltage on winding N_2 is higher than the $|V_{o2}|$, the diode D_2 is reverse biased while the body diode of Q_2 is forward biased. Vice versa, if the voltage on winding N_2 is lower than $|V_{o2}|$, the diode D_2 is forward biased while the body diode of Q_2 is reverse biased. Therefore, the voltage stress on D_2 and Q_2 can be expressed as:

$$V_{D2[t_0-t_1]} = \max\left\{V_{in\_rec} \times \frac{N_2}{N_1} - |V_{o2}|, 0\right\} \tag{6}$$

$$V_{Q_2\_ds[t_0-t_1]} = \max\left\{|V_{o2}| - V_{in\_rec} \times \frac{N_2}{N_1}, 0\right\} \tag{7}$$

Since both V_{in} and the output V_{o2} are not constant in a half line cycle, the polarity of the diode D_2 and the body diode of Q_2 during [t_0-t_1] change in a half line cycle. It is also shown in Fig. 5 with dotted lines that the voltage V_{D2} and V_{Q2_ds} have two possible scenarios.

B. Time Interval [t_1-t_2]

As the MOSFET Q_1 is turned off at time t_1, the magnetic current is forced to conduct in diode D_1. The voltage across the winding N_1 is clamped to be the same as the output V_{o1} (ignore the forward voltage drop of diode D_1). The diode D_3 is forward biased while the voltage on the MOSFET Q_1 is the sum of input voltage and output voltage V_{o1}, and can be expressed as:

$$V_{Q_1\_ds[t_1-t_2]} = V_{in\_rec} + V_{o1} \tag{8}$$

During this time interval, the energy stored in the inductor is transferred to the output V_{o1}. The magnetic current in winding N_1 starts decreasing at time t_1 and becomes zero at time t_2, which ends the phase one operation. The diode D_2 is forward biased while the body diode of Q_2 is reverse biased during this time interval. The voltage across the drain to source terminals of Q_2 can be expressed as:

$$V_{Q_2\_ds[t_1-t_2]} = V_{N_2[t_1-t_2]} + |V_{o2}| = V_{o1} \times \frac{N_2}{N_1} + |V_{o2}| \tag{9}$$

C. Time Interval [t_2-t_3]

The phase two operation starts at time t_2 when the MOSFET Q_2 is turned on and the switching current in winding N_2 starts increasing from zero. The switching current in Q_2 and D_2 peaks at time t_3 right before Q_2 is turned off and can be expressed as:

$$I_{Q_2\_t_3} = I_{D_2\_t_3} = \frac{|V_{o2}| \times (t_3 - t_2)}{L_{N2}} \tag{10}$$

Where in (10), L_{N2} represents the inductance of the winding N_2. Since V_{o2} is negative, the dot end of the winding N_1 has lower potential. Therefore, the diode D_1 is reverse biased and the voltage across it can be expressed as:

$$V_{D_3[t_2-t_3]} = \max\left\{|V_{o2}| \times \frac{N_2}{N_1} - V_{in\_rec}, 0\right\} \tag{11}$$

$$V_{Q_1\_ds[t_2-t_3]} = \max\left\{V_{in\_rec} - |V_{o2}| \times \frac{N_2}{N_1}, 0\right\} \tag{12}$$

As also indicated in Fig. 5 with a dotted line, the voltage V_{D3} and the voltage V_{Q1_ds} have two possible scenarios during this time interval.

D. Time Interval [t_3-t_4]

After Q_2 is turned off at time t_3, the magnetic current commutes from winding N_2 to winding N_1. The voltage on the winding N_2 is clamped at voltage V_{o1}. The inductor releases stored energy back to the output V_{o1} and the current in D_1 decreases. The voltage across each component is the same as in the time interval [t_1-t_2]. The peak current in the output diode D_1 can be expressed as:

$$I_{D_{1t_3}} = \frac{N_2}{N_1} \times I_{Q_{2t_3}} = \frac{N_2}{N_1} \times \frac{|V_{o2}| \times (t_3 - t_2)}{L_{N2}} = \frac{|V_{o2}| \times (t_3 - t_2)}{L_{N1}} \times \left(\frac{N_1}{N_2}\right) \tag{13}$$

This interval ends at t_4 when the current in D_1 drops to zero.

E. Time Interval [t_4-t_5]

This is a small time interval needed to maintain discontinuous current mode (DCM) operation. No active switching operation occurs in this time interval.

III. Control Strategy

Fig. 6 shows the control diagram of the proposed MEC LED driver. Two control loops are needed for the LED driver, namely the LED current feedback loop and the output V_{o2} voltage loop. A constant in a half line cycle. Therefore, the on time of Q_1 during phase one operation, (t_1-t_0), is a constant and the phase one input current automatically follows the input voltage to perform the power factor correction. When the sensed input current is not equal to the LED current reference, V_{ctrl1} will be changed automatically by the feedback loop. Therefore, (t_1-t_0) and the RMS input current will change. The change with RMS input current changes the input power and the output voltage V_{o1}. V_{o1} will settle where it can produces the exact LED current required by its reference. It should be noted that the average voltage of V_{o2} is a constant in the design, and it is not a part of the LED current regulation loop. To achieve ripple cancellation, the output voltage V_{o1} is sensed by the low-frequency sensing (LFS) circuit to extract the double-line-frequency ripple voltage. With proper conditioning, the sensed ripple voltage becomes the reference voltage of V_{o2}, V_{o2_ref}. The output voltage V_{o2} is sensed and compared with its reference.

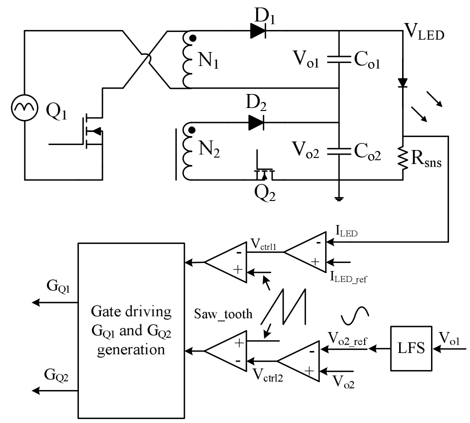

Fig. 6 Control diagram of the proposed multiplexing energy channeling LED driver

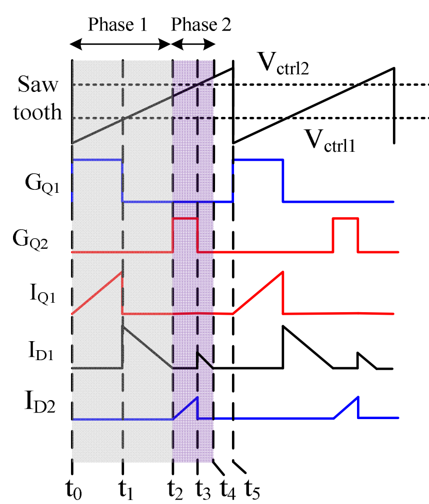

Fig. 7 Gate driving generating scheme of the multiplexing energy channelling LED driver

The compensated error voltage V_{ctrl2} is compared with the same saw tooth signal to produce the gate driving signal of Q_2 during the phase two operation. With a well-designed regulation loop, the output V_{o2} will tightly follow the reference voltage and produce an opposite ripple voltage to cancel the ripple from V_{o1}.

IV. Experimental Verification

To verify the proposed MEC LED driver, a 7.5W experimental prototype was built and tested. Table 1 shows the design specifications and the circuit parameters of the experimental prototype.

TABLE 1 DESIGN SPECIFICATIONS AND CIRCUIT PARAMETERS

Design Specification	
Input Voltage	89Vrms – 132Vrms
V_{LED}	~ 50V
I_{LED}	0.15A

Circuit Parameter	
Coupled inductor	N_1: N_2 = 8:1, L_{N1}=1.25mH EE16 core
Main MOSFET Q_1	2SK2803 (450V 3A)
Main output diode D_1	LQA06T300 (300V 6A)
MOSFET Q_2	ZXMN4A06GTA (40V 5A)
Output diode D_2	MBRS340T3G (40V 4A)
Block diode D_3	MBRS340T3G (40V 4A)
Output capacitor C_{o1}	EKZN101ELL151MJ25S (150μF, 100V)
Output capacitor C_{o2}	CL21A226KOQNNNE (22μF, 16V)
Controller	PIC16F1578-I/SS
Switching frequency f_s	20kHz

Fig. 8 shows the key ripple cancellation waveforms of the proposed MEC LED driver. There is a 3Vpk-pk 120Hz ripple voltage generated at the output Vo1. An opposite ripple voltage is generated at the output V_{o2}. Because of ripple cancellation between V_{o1} and V_{o2}, the overall LED voltage has a much smaller ripple than that of V_{o1}. The 120Hz ripple current is measured to be 25mA peak to peak, which means 12.5mA peak and is 8.3% of the average 150mA LED current.

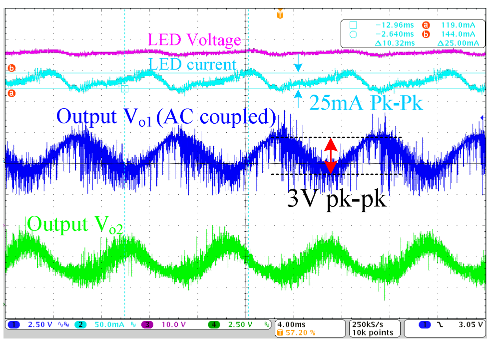

Fig. 8 Ripple cancellation waveforms of the MEC LED driver

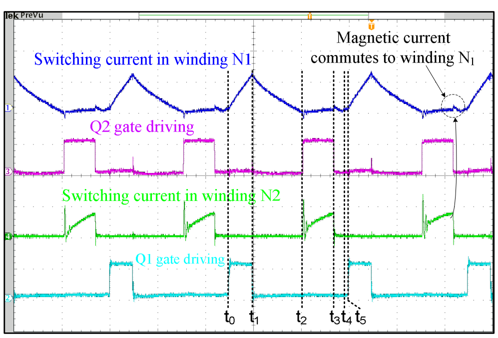

Fig. 9 Critical switching waveforms show gating time and switching currents

Fig. 9 shows the gate driving and the switching current waveforms. A switching cycle starts at time t_0 when the MOSFET Q_1 is turned on. The magnetic current in winding N_1 (and Q_1) starts rising from zero. The magnetic current peaks at t_1 when Q_1 is turned off and continues flowing in D_1. The magnetic current drops to zero at time t_2, which ends the phase one operation. The MOSFET Q_2 is turned on at t_2 and the magnetic current in winding N_2 (and Q_2/D_2) starts increasing from zero. The current peaks at t_3 when Q_2 is turned off. The magnetic current then commutes from winding N_2 to winding N_1 and continues its flow in diode D_1. A small bump on the switching current waveform of N_1 represents the current in diode D_1 after Q_2 is turned off. The magnetic current in winding N_1 drops to zero at time t_4, which ends the phase two operation.

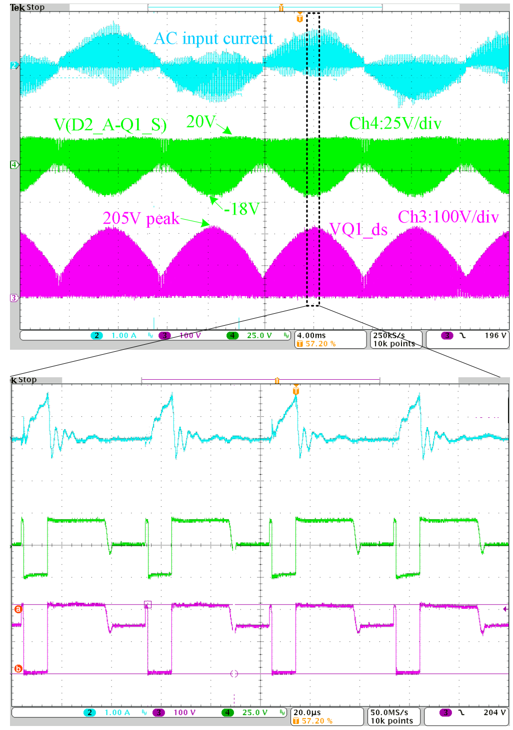

Fig. 10 Components voltage stresses under 110Vrms input, 50V LED voltage output

Fig. 10 shows the voltage stresses of the power components under 110Vrms input and 50V LED output. The maximum voltage stress across the drain and source of Q_1 is around 205V under 110Vrms input. The voltage between the anode terminal of D_2 and the source terminal of Q_2, $V_{(D2\_A\text{-}Q2\_S)}$, is measured. The upper boundary of the waveform represents the voltage stresses of the body diode of Q_2 as D_2 is currently forward biased. Therefore, the maximum voltage across the drain to source of Q_2 is around 20V. The lower boundary of the waveform represents the voltage stresses on the diode D_2 since the body diode of Q_2 is forward biased. The maximum voltage stress on D_2 is around 18V. The voltage stresses of Q_2 and D_2 are quite small and low voltage rating devices can be used.

Fig. 11 shows the efficiency comparison between the proposed MEC LED driver and a conventional Buck-Boost LED driver. The efficiency of the proposed LED driver is approximately 2% below the efficiency of a conventional Buck-Boost LED driver, which is a small price to pay when achieving flicker-free LED driving and a significant reduction on storage capacitor C_{o1}.

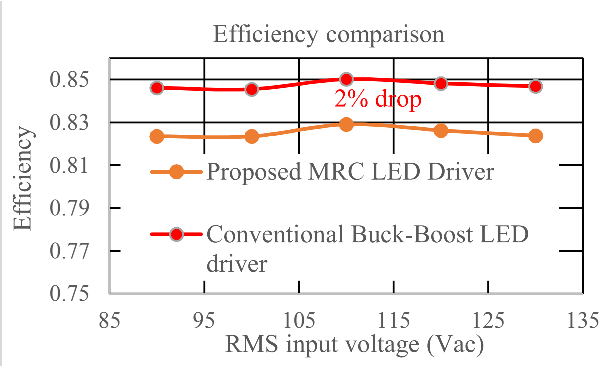

Fig. 11 Efficiency comparison between the proposed MRC LED driver and a conventional Buck-Boost LED driver under full load condition

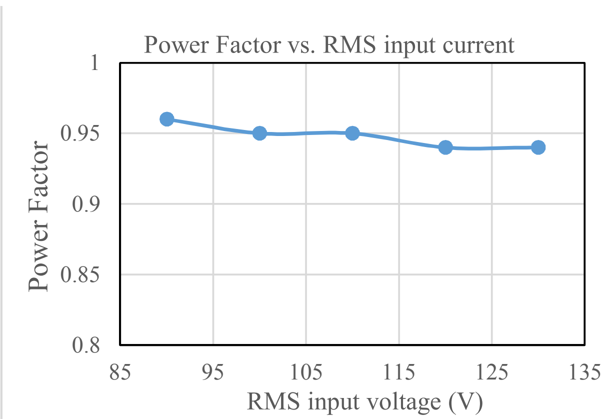

Fig. 12 Power Factor Correction performance of the proposed multiplexing energy channeling LED driver

Fig. 12 shows the power factor correction performance of the proposed MEC LED driver. Around 0.95PF has been achieved under full load condition.

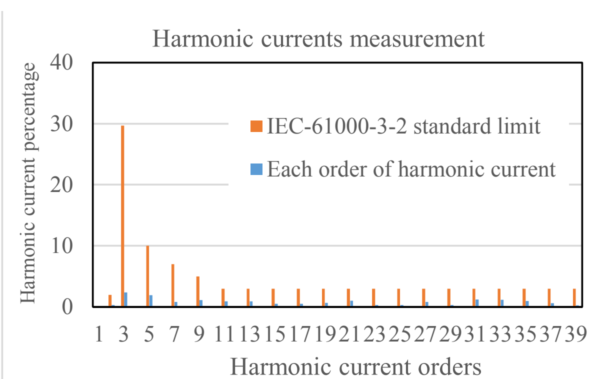

Fig. 13 AC input harmonic current measurement

Fig. 13 shows the AC input harmonic currents of the proposed multiplexing energy channeling LED driver. All orders of harmonic content stay far below the IEC-61000-3-2 limit.

Fig. 14 shows the photo of the experimental prototype.

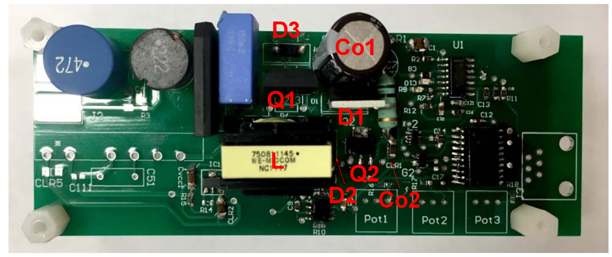

Fig. 14 7.5W multiplexing energy channeling LED Driver experimental prototype

V. Conclusion

A MRC LED driver has been proposed in this paper to achieve flicker-free LED driving performance with reduced storage capacitor and high power factor correction. The power circuit operates in a time multiplexing manner, which achieves power delivery and ripple cancellation in two different time periods of one switching cycle. Compared to previous ripple cancellation LED drivers, the new design eliminates the need of using a separate ripple cancellation converter to achieve flicker-free LED driving performance , which further reduces cost and will be preferred in low power, cost sensitive, applications. A 7.5W experimental prototype had been built and tested to verify the operation of the LED driver. The experimental prototype achieves 0.95PF, 8% of double-line-frequency ripple LED current performance while it is only 2% lower efficiency than a conventional Buck-Boost LED driver. Overall, the experimental results are very promising and highly agree with the analysis.

References

[1] LED Lighting Market by Installation Type (New Installation and Retrofit Installation), End-Use Application (Indoor Lighting and Outdoor Lighting), Product Type (Lamps and Luminaires), and Geography - Global Forecast to 2022 . (2017, January). Retrieved June 20, 2017, from http://www.marketsandmarkets.com/Market-Reports/led-lighting-market-201130554.html?gclid=EAIaIQobChMIjs_0uu3N1AIVgrfACh2J2wJnEAAYASAAEgKXBfD_BwE

[2] ENERGY STAR Program Requirements for Solid State Lighting Luminaires, Version 1.1 , December 19, 2008.

[3] B. Lehman, A.J. Wilkins, "Designing to Mitigate Effects of Flicker in LED Lighting: Reducing risks to health and safety," in IEEE Power Electronics Magazine, Vol 1, No 3, September 2014. pp. 18-26.

[4] X.B. Ruan, B.B. Wang, K. Yao and S. Wang, "Optimum Injected Current Harmonics to Minimize Peak-to-Average Ratio of LED Current for Electrolytic Capacitor Less AC–DC Drivers" in IEEE Transactions on Power Electronics, Vol. 26, No. 7, pp.1820-1825, July 2011.

[5] B.B. Wang, X.B. Ruan, K. Yao and M. Xu, "A Method of Reducing the Peak-to-Average Ratio of LED Current for Electrolytic Capacitor-Less AC–DC Drivers," in IEEE Transactions on Power Electronics, Vol. 25, No. 3, pp.592-601, March 2010.

[6] D. G. Lamar, J. Sebastian, M. Arias and A. Fernandez, "On the Limit of the Output Capacitor Reduction in Power-Factor Correctors by Distorting the Line Input Current," in IEEE Transactions on Power Electronics, Vol. 27, No. 3, pp. 1168-1176, March 2012.

[7] Y.C. Li and C.L. Chen, "A Novel Primary-Side Regulation Scheme for Single-Stage High-Power-Factor AC–DC LED Driving Circuit," in IEEE Transactions on Industrial Electronics, Vol. 60, No. 11, pp.4978-4986, November 2013.

[8] X.G. Xie, J. Wang, C. Zhao, Q. Lu and S.R. Liu, "A Novel Output Current Estimation and Regulation Circuit for Primary Side Controlled High

Power Factor Single-Stage Flyback LED Driver," in IEEE Transactions on Power Electronics, Vol. 27, No. 11, pp. 4602-4612, November 2012.

[9] H.H. Chou, Y.S. Hwang and J.J. Chen, "An Adaptive Output Current Estimation Circuit for a Primary-Side Controlled LED Driver," IEEE Transactions on Power Electronics, Vol.28, No.10, Oct. 2013, pp.4811,4819

[10] J.M. Zhang, H.L. Zeng and T. Jiang, "A Primary-Side Control Scheme for High-Power-Factor LED Driver With TRIAC Dimming Capability," IEEE Transactions on Power Electronics, Vol.27, No.11, Nov.2012, pp.4619,4629,

[11] S. Wang, X.B. Ruan, K. Yao, S.C. Tan, Y. Yang and Z.H. Ye, "A Flicker-Free Electrolytic Capacitor-Less AC–DC LED Driver" in IEEE Transactions on Power Electronics, Vol. 27, No. 11, pp.4540-4548, November 2012.

[12] Y. Yang, X.B. Ruan, L. Zhang, J.X He and Z.H Ye, "Feed-Forward Scheme for an Electrolytic Capacitor-Less AC/DC LED Driver to Reduce Output Current Ripple," in IEEE Transactions on Power Electronics, Vol. 29, No. 10, pp. 5508-5517, Octorber 2014.

[13] P. T. Krein, R. S. Balog and M. Mirjafari, "Minimum Energy and Capacitance Requirements for Single-Phase Inverters and Rectifiers Using a Ripple Port," in IEEE Transactions on Power Electronics, Vol. 27, No. 11, pp. 4690-4698, November. 2012.

[14] Q.C. Hu and R. Zane, "Minimizing Required Energy Storage in Off-Line LED Drivers Based on Series-Input Converter Modules," in IEEE Transactions on Power Electronics, Vol. 26, No. 10, pp.2887-2895, October 2011.

[15] C.A. Cheng, C.H. Chang, T.Y. Chung and F.L. Yang, "Design and Implementation of a Single-Stage Driver for Supplying an LED Street-Lighting Module With Power Factor Corrections," in IEEE Transactions on Power Electronics, Vol. 30, No. 2, pp. 956-966, February 2015.

[16] J. C. W. Lam and P. K. Jain, "Isolated AC/DC Offline High Power Factor Single-Switch LED Drivers Without Electrolytic Capacitors," in IEEE Journal of Emerging and Selected Topics in Power Electronics, Vol. 3, No. 3, pp. 679-690, September 2015.

[17] J. C. W. Lam and P. K. Jain, "A High Power Factor, Electrolytic Capacitor-Less AC-Input LED Driver Topology With High Frequency Pulsating Output Current," in IEEE Transactions on Power Electronics, Vol. 30, Vo. 2, pp. 943-955, Feburary 2015.

[18] Z. Bo, Y. Xu, X. Ming, Q.L. Chen and Z.A. Wang, "Design of Boost-Flyback Single-Stage PFC converter for LED power supply without electrolytic capacitor for energy-storage," in International Power Electronics and Motion Control Conference, Wuhan, 2009.

[19] K. M. Divya and R. Parackal, "High power factor integrated buck-boost flyback converter driving multiple outputs," in Online International Conference on Green Engineering and Technologies, Coimbatore, 2015

[20] D.Camponogara, D.R.Vargas, M.A.Dalla Costa, J.M.Alonso, J.Garcia and T.Marchesan, "Capacitance reduction with an optimized converter connection applied to LED drivers," in IEEE Transactions on Industrial Electronics, Vol. 62, No.1, pp.184-192, January 2015.

[21] D.Camponogara, G.F.Ferreira, A. Campos, M.A. Dalla Costa and J. Garcia, "Offline LED Driver for Street Lighting With an Optimized Cascade Structure," in IEEE Transactions on Industry Applications, Vol.49, No 6, pp.2437-2443, December 2013.

[22] P. Fang, Y. j. Qiu, H. Wang and Y. F. Liu, "A Single-Stage Primary-Side-Controlled Off-line Flyback LED Driver with Ripple Cancellation," in IEEE Transactions on Power Electronics, Vol. 32, no. 6, pp. 4700-4715, June 2017.

[23] Y. Qiu, L. Wang, H. Wang, Y. F. Liu and P. C. Sen, "Bipolar Ripple Cancellation Method to Achieve Single-Stage Electrolytic-Capacitor-Less High-Power LED Driver," in IEEE Journal of Emerging and Selected Topics in Power Electronics, vol. 3, no. 3, pp. 698-713, Sept. 2015.

[24] P. Fang, Y. F. Liu and P. C. Sen, "A Flicker-Free Single-Stage Offline LED Driver With High Power Factor," in IEEE Journal of Emerging and Selected Topics in Power Electronics, vol. 3, no. 3, pp. 654-665, Sept. 2015.

[25] P. Fang and Y. F. Liu, "Energy Channeling LED Driver Technology to Achieve Flicker-Free Operation with True Single Stage Power Factor Correction," in IEEE Transactions on Power Electronics, vol. 32, no. 5, pp. 3892-3907, May 2017.

[26] F.H. Zhang, J.J.Ni and Y.J.Yu, "High Power Factor AC–DC LED Driver With Film Capacitors," in IEEE Transactions on Power Electronics, Vol. 28, No. 10, pp. 4831-4840, October 2013.

[27] W. Chen and S.Y.R. Hui, "Elimination of an Electrolytic Capacitor in AC/DC Light-Emitting Diode (LED) Driver With High Input Power Factor and Constant Output Current," in IEEE Transactions on Power Electronics, Vol. 27, No. 3, pp. 1598-1607, March 2012.

[28] H. Ma, J. S. Lai, Q. Feng, W. Yu, C. Zheng and Z. Zhao, "A Novel Valley-Fill SEPIC-Derived Power Supply Without Electrolytic Capacitor for LED Lighting Application," in IEEE Transactions on Power Electronics, Vol. 27, No. 6, pp. 3057-3071, June 2012.

[29] U. Ramanjaneya Reddy and B. L. Narasimharaju, "Single-stage electrolytic capacitor less non-inverting buck-boost PFC based AC–DC ripple free LED driver," in IET Power Electronics, vol. 10, no. 1, pp. 38-46, 2017.

[30] Y.Q. Hu, L. Huber, M.M. Jovanović, "Single-Stage, Universal-Input AC/DC LED Driver With Current-Controlled Variable PFC Boost Inductor," in IEEE Transactions on Power Electronics, Vol. 27, No. 3, pp.1579-1588, March 2012.

[31] Y.C. Li and C.L Chen, "A Novel Single-Stage High-Power-Factor AC-to-DC LED Driving Circuit With Leakage Inductance Energy Recycling," in IEEE Transactions on Industrial Electronics, Vol. 59, No. 2, pp.793-802, February 2012.

[32] R.H. Zhang, H.S. Chung, "A TRIAC-Dimmable LED Lamp Driver With Wide Dimming Range," in IEEE Transactions on Power Electronics, Vol. 29, No. 3, pp. 1434-1446, March 2014.